

Zircaloy Thermal Conductivity

Preliminary Recommendation

The preliminary recommendation equation for the thermal conductivity of Zircaloy is

$$\lambda = 12.767 - 5.4348 \times 10^{-4} T + 8.9818 \times 10^{-6} T^2 \quad (1)$$

where λ is the thermal conductivity in $\text{W m}^{-1} \text{K}^{-1}$ and T is the temperature in K. This equation was obtained from a least squares analysis of the available thermal conductivity and thermal diffusivity data on Zircaloy-2 and Zircaloy-4. Figure 1 compares the values of the thermal conductivity obtained from this equation with the Zircaloy-2 and Zircaloy-4 data included in the analysis. One standard deviation uncertainty bands have been included in the figure. This equation is valid for the temperature range 300 to 1800 K. Extrapolation to higher temperatures, where no data are available, is not recommended because it is a polynomial fit to the data, not a physically-based equation. Tabulated values of the thermal conductivity calculated from Eq.(1) are given in Table 1.

Uncertainty

Figure 1 shows the one standard deviation uncertainties for the recommended equation. They increase with temperature from 4% at 300 K to 5% at 500 K, 6% at 800 K and 7% at 1200 K. Average uncertainties from 1200 to 1800 K are 7%.

Discussion

Review of Thermal Conductivity Data

Table 2 lists the measurements of the thermal conductivity of Zircaloy-2 and Zircaloy-4 in chronological order and gives the year of measurement, the temperature range, and number of data. Data from 1958 through 1966, which includes the data of Lucks and Deem [1], Chirigos et al.[2], Powers [3], Anderson et al. [4], Scott [5], and Feith [6] were used in the development of the MATPRO equation [10] for the thermal conductivity of Zircaloy. The MATPRO equation for the thermal conductivity of Zircaloy is

$$\lambda = 7.51 + 2.09 \times 10^{-2} T - 1.45 \times 10^{-5} T^2 + 7.67 \times 10^{-9} T^3 \quad (2)$$

where λ is the thermal conductivity in $\text{W m}^{-1} \text{K}^{-1}$ and T is the temperature in K. In Figure 2, the MATPRO equation is shown with these data that were included in its derivation. In addition to the data listed in Table 2, the MATPRO manual [10] lists Zircaloy-2 data given by Chirigos et al. [2] and an additional set of data for Zircaloy-2 data reported by Powers [3]. Examination of these data [2,3] showed that both sets of data are from measurements at the Battelle Memorial Institute and are identical to the data reported by Lucks and Deem [1]. Inclusion of these duplicate sets of data in the derivation of the MATPRO equation had the effect of weighting the data of Lucks and Deem by a factor of three. More recent data tabulated in the 1997 IAEA technical document “Thermophysical Properties of Materials for Water Cooled Reactors” [7] are the Atomic Energy of Canada Limited (AECL) data reported by Price [8] and Mills et al. [9] and new measurements by the Institute of Atomic Energy of China. Figure 3, which compares these new data with the MATPRO equation and the older data fit by the MATPRO equation, indicates that some of the AECL data [7-9] are high relative to the MATPRO equation. However, some of the data fit by the MATPRO equation are also high relative to the MATPRO equation.

Review of Thermal Diffusivity Data

No thermal diffusivity data were considered in the formulation of the MATPRO equation. In 1970, Wheeler [11] reported anomolous results of thermal diffusivity measurements on Zircaloy-2 using a modulated electron beam technique. These measurements gave thermal diffusivities that were constant in the temperature range from 550 to 925 K but varied with the thickness of the sample. Walter et al. [12] studied effects of sample orientation and thickness on thermal diffusivity of Zircaloy-2 plate. Although no difference in the thermal diffusivity was observed for specimens from different directions, thickness effects were detected in measurements made at Harwell using thermocouples but not in measurements at Manchester that used infrared detectors. These results are shown in Figure 4, where H indicates Harwell measurements using thermocouples and M denotes

the Manchester measurements using an infrared detector. Sample thickness has been included in the legend. Based on results of these measurements, the Wheeler data [11] and the Harwell data on small samples reported by Walter et al. [12] have not been included in this analysis. The Manchester data and the data from Harwell on 2 mm samples are consistent with later measurements on Zircaloy-2 and Zircaloy-4 by Murabayashi et al. [13], by Taylor [14], and by Maglic [15].

Thermal diffusivity data for unoxidized Zircaloy-2 and Zircaloy-4 are listed in chronological order in Table 3 and shown in Figure 5. Figure 5 shows that although the data of Gilchrist et al. [16] are consistent with the AECL data [7-9] for the thermal diffusivity of an annealed rod in the axial direction, these data are higher than other diffusivity data.

Data on the effects of oxidation on the thermal diffusivity of Zircaloy-2 and Zircaloy-4 [16 -20] are not being included in this analysis, which is to determine the thermal conductivity of unoxidized Zircaloy. In their oxidation studies, Gilchrist [16, 17], Peggs et al. [18] and Bunnell et al. [19, 20] also report results of thermal diffusivity measurements on samples that were not oxidized in steam. Peggs et al. report no measurement data but show curves for the thermal diffusivities of a Zircaloy-2 tube in the radial direction, a Zircaloy-2 calandria tube, and a Zircaloy-4 fuel sheath. In Figure 6, the curves reported by Peggs et al. are compared with the low-temperature thermal diffusivity data listed in Table 3. It shows that the results reported by Peggs et al. are consistently higher than other data and appear to have a different slope indicating either a systematic error or differences due to the condition of the surface. Thus, these results reported by Peggs et al. have not been included in this analysis. In Figure 7, the data of Bunnell et al. [19,20] for as received samples of Zircaloy-4 tube, Zircaloy-4 bar, and Zircaloy-2 and the fits to these data by Bunnell et al. [19,20] are compared with the thermal diffusivity data listed in Table 3. Although some of the data of Bunnell et al. are in the same range as other data, the recommended curves of Bunnell et al. are consistently low compared to other data. Thus, the data and equations of Bunnell et al. have not been included in this analysis.

Data Analysis

The temperatures for all data obtained prior to 1968 were converted from the 1948 International Practical Temperature Scale (IPTS) to the 1968 IPTS. Thermal diffusivity data have been converted to thermal conductivity using the equation

$$\lambda = D C_p \rho \quad (3)$$

where λ is the thermal conductivity, D is the thermal diffusivity, C_p is the heat capacity, and ρ is the density. The heat capacity has been calculated from equations for the heat capacity of Zircaloy-2. For the α - phase, from $273 \text{ K} < T < 1100 \text{ K}$,

$$C_p = 255.66 + 0.1024 T \quad (4)$$

where temperature is in K and the heat capacity is in $\text{J kg}^{-1} \text{ K}^{-1}$. For the β -phase from $1320 \text{ K} < T < 2000 \text{ K}$

$$C_p = 597.1 - 0.4088 T + 1.565 \times 10^{-4} T^2 \quad (5)$$

where temperature is in K and heat capacity is in $\text{J kg}^{-1} \text{ K}^{-1}$. From 1100 K through 1214 K, in the $(\alpha + \beta)$ - phase-transition region, the heat capacity of Zircaloy-2 has been calculated from the sum of Eq.(4) and a Gaussian function that represents the peak of the transition. This Gaussian function is:

$$f(T) = 1058.4 \exp\left[\frac{(T-1213.8)^2}{719.61}\right] \quad (6)$$

where temperature is in K and $f(T)$ is in $\text{J kg}^{-1} \text{ K}^{-1}$. From 1214 to 1320 K, the heat capacity of Zircaloy-2 is calculated from the sum of Eq.(5) + Eq.(6).

The Zircaloy density as a function of temperature has been calculated from the room temperature

density, 6501 kg m^{-3} , and the change in volume obtained from the linear thermal expansion in three orthogonal directions. For the α -phase ($T < 1083 \text{ K}$), the calculated densities are well represented by the linear equation

$$\rho = 6595.2 - 0.1477 T \quad (7)$$

where ρ is the density in kg m^{-3} and T is the temperature in K. The change in density through the ($\alpha + \beta$)- phase-transition region was set equal to 0.67%, the value recommended for zirconium by Guillermet [21]. In the β -phase (1144 - 1800 K), the density has been calculated from the linear equation

$$\rho = 6690. - 0.1855 T \quad (8)$$

where ρ is the density in kg m^{-3} and T is the temperature in K.

Figure 8 shows both the thermal conductivity and thermal diffusivity data expressed as thermal conductivity. Some of the low-temperature AECL data and the data of Scott and of Gilchrist appear high relative to other data in the same temperature range. In Figure 9, the MATPRO equation is compared with the data fit by the MATPRO equation, the more recent thermal conductivity data, and the thermal conductivities obtained from the thermal diffusivity measurements. It shows that from 400 to 1200 K, the MATPRO equation is high relative to data from thermal diffusivity measurements.

Because much new data have been obtained since the derivation of the MATPRO equation and the MATPRO equation is not a good representation of all these data, a new analysis has been completed to determine a new equation for the thermal conductivity of Zircaloy. The thermal conductivity and thermal diffusivity data listed in Tables 2 and 3 have been considered in this analysis. To determine if some of the sets of data listed in Tables 2 and 3 and shown in Figure 8 do not belong to the same statistical set and should not be included in the final analysis, all the data shown in Figure 8 were

fit to a quadratic function by a least squares analysis. This quadratic equation

$$\lambda = 13.09 - 7.920 \times 10^{-4} T + 9.043 \times 10^{-6} T^2 \quad (9)$$

represents the common consensus of all the data. The data, quadratic fit, and error bands at two standard deviations from the quadratic fit are shown in Figure 10. Sets of data that have points outside these error bands have been identified in the legend and are shown as filled symbols in the graph. The high datum in Figure 10 at 925 K is from measurements by Feith [6]. The two unusually low data at approximately 1140K are from measurements by Maglic et al. [15]. These data, which are obviously bad points, have not been included in the final analysis.

To determine how well each set of data are represented by the MATPRO equation and by the quadratic fit, modified variances relative to the MATPRO equation and the quadratic fit were calculated for each set of data. These modified variances, σ^2 , are defined as

$$\sigma^2 = \frac{1}{N} \sum [\lambda_{Eq}(T_i) - \lambda(T_i)]^2 \quad (10)$$

where N is the number of points in the data set, $\lambda_{Eq}(T_i)$ is the thermal conductivity at temperature T_i determined by the MATPRO equation or the quadratic fit, and $\lambda(T_i)$ is a data point in the data set. These modified variances are given in Tables 2 and 3 for each set of data. Sets of data for which the majority of points fell outside two standard deviations and/or for which the modified variance of the quadratic equation, Eq. (9), is greater than 2.5 have been excluded from the final analysis. Data excluded from the analysis are shown in Figure 11. Thermal conductivity measurements not included are data sets AECL4 Zircaloy-2 cold-worked tube, AECL5 Zircaloy-2 annealed strip in the transverse direction, AECL6 Zircaloy-2 stress-relieved thin-wall tube in the circumferential direction, and AECL7 Zircaloy-2 annealed rod. Thermal diffusivity data excluded from this analysis are the AECL3d Zircaloy-2 annealed rod in the axial direction and the 1976 Zircaloy-2 measurements of Gilchrist. Although only one datum of Gilchrist falls outside the two standard

deviations, these data clearly have a different temperature behavior than the data included in the final analysis. For example, the data of Gilchrist [16] show a distinct discontinuity at the phase transition that is not evident in thermal conductivities obtained from other measurements. The low-temperature data of Gilchrist are high with a different slope from the common consensus. These deviations of the Gilchrist data from the common consensus are illustrated by modified variances of 2.5 and 2.7, respectively relative to the MATPRO equation and the quadratic fit.

The final analysis include 321 points from the data sets listed in Table 4. Because the number of data obtained by the measurements by Maglic et al. are considerably higher than that of any other investigator, these data were reduced to 53 points by averaging the temperatures and thermal conductivities of data that were obtained at nearly the same temperature. This prevented excessive weighting of the measurements by Maglic et al. in the final analysis.

Table 5 Regression Statistics for Fits to Zircaloy Thermal Conductivity

Statistic/Functional Form	Cubic	Quadratic	Quadratic + 1/T	MATPRO
χ^2	230	234	233	322
Free parameters	4	3	4	4
Variance	0.725	0.736	0.736	1.017
Standard Deviation	0.851	0.858	0.858	1.008

The data listed in Table 4 were fit using multiple regression analysis to three functional forms: quadratic, cubic, and quadratic + 1/T. The quadratic + 1/T functional form was included because Fink and Leibowitz [22] found that it provided the best fit to the thermal conductivity of zirconium. The goodness of fit for each functional form is shown in Table 5, which gives χ^2 (the sum of the squares of the deviation of the data from the fit), the variance ($\chi^2/[N-\text{free parameters}]$, where N= the number of points), and the standard deviation. For completeness, these statistics for the MATPRO equation have also been included in Table 5. All the new equations fit the data

considerably better than the MATPRO equation. Because the statistics given in Table 5 indicate that the quadratic + 1/T form does not fit the data any better than the quadratic equation, this functional form has been excluded from further consideration. The quadratic equation referred to in Table 4 and 5 is Eq.(1). The cubic equation is:

$$\lambda = 11.498 + 4.6765 \times 10^{-3} T + 2.761 \times 10^{-6} T^2 + 2.2147 \times 10^{-9} T^3 \quad (11)$$

where λ is the thermal conductivity in $\text{W m}^{-1} \text{K}^{-1}$ and T is the temperature in K. The MATPRO equation is Eq.(2).

The data included in this analysis are compared with the cubic [Eq.(11)], quadratic [Eq.(1)], and MATPRO [Eq.(2)] equations in Figure 12. Figure 13 shows the deviations of the data from the cubic and quadratic equations. Examination of Figures 12 and 13 shows that the cubic equation improvement is mainly from better fitting of the high-temperature points. In fact, some low-temperature data are better fit using the quadratic form. Table 4 gives the modified variances defined according to Eq. (10) for each set of data relative to the MATPRO equation and the quadratic and cubic equations. It shows that the cubic equation provides better fits than the quadratic equation for the data of Lucks and Deem, Anderson, Scott, Feith, and Taylor and the AECL thermal conductivity data. Although the cubic equation provides slightly better fits to some sets of data and to the highest temperature points, an F test comparing the quadratic and cubic fits of these data shows that the additional term in the cubic equation is not statistically justified. Therefore, the quadratic equation, Eq. (1) that fits the combined thermal conductivity and thermal diffusivity data has been recommended.

References

1. C. F. Lucks and H. W. Deem, "Progress Relating to Civilian Applications During June 1958: Thermal Conductivity of Uranium and UO_2 ," USAEC Report **BMI-1273**, 1-62 (1958).
2. J. N. Chirigos, S. Kass, W. W. Kirk, and G. J. Salvaggio, *Development of Zircaloy-4*, in Fuel Element Fabrication with Special Emphasis on Cladding Materials, Proceedings of a Symposium held in Vienna, May 10-13, 1960, Vol. 1, pp. 19-56, Academic Press, London for the International Atomic Energy Agency (1961).
3. A. E. Powers, *Application of the Ewing Equation for Calculating Thermal Conductivity from Electrical Conductivity*, Knolls Atomic Power Laboratory of General Electric Report **KAPL-2146**, (April 7, 1961).
4. W. K. Anderson, C. J. Beck, A. R. Kephart, and J. S. Theilacker, "Zirconium Alloys," Reactor Structural Materials: Engineering Properties as Affected by Nuclear Reactor Service, ASTM-STP-314 (1962), pp. 62-93; as referenced in "SCDAP/RELAP5/MOD 3.1 Code Manual: MATPRO - A Library of Materials Properties for Light-Water-Reactor Accident Analysis, **NUREG/CR-6150, EGG-2720 Vol. 4** (1995).
5. D. B. Scott, "Physical and Mechanical Properties of Zircaloy 2 and 4", USAEC Report **WCAP-3269-41**, 1-68 (1965).
6. (A. D. Feith), "High-Temperature Materials Program: Property Measurements," USAEC Report **GEMP-61**, 153-155 (1966). C. G. Collins, pp 157-169
7. J. Cleveland (ed.), "Thermophysical Properties of Materials for Water Cooled Reactors, International Atomic Energy Agency Report **IAEA-TECDOC-949**, pp. 77 (June 1997).
8. E. G. Price, "Thermal Conductivity, Electrical Resistivity, and Specific Heat of CANDU Construction Alloys and AISI Type 403 End Fitting," AECL Report **TDVI-3680** (1980), as tabulated in "Thermophysical Properties of Materials for Water Cooled Reactors, J. Cleveland (ed.), International Atomic Energy Agency Report **IAEA-TECDOC-949**, p. 78 (June 1997).
9. R. W. Mills, M. H. Schankula, B. A. Lange, "The Thermal Conductivity of Zirconium, Zircaloy-2, and Zirconium-2.5 wt% Niobium and some of Their Hydrides from 150°C to 350°C," AECL Internal Document, as tabulated in "Thermophysical Properties of Materials for Water Cooled Reactors, J. Cleveland (ed.), International Atomic Energy Agency Report **IAEA-TECDOC-949**, p. 78 (June 1997).

10. D. T. Hagrman, ed., "SCDAP/RELAP5/MOD 3.1 Code Manual: MATPRO - A Library of Materials Properties for Light-Water-Reactor Accident Analysis, **NUREG/CR-6150, EGG-2720 Vol. 4** (1995).
11. M. J. Wheeler, *Some Anomalous Thermal Diffusivity Results on Hafnium, Niobium and Zircaloy 2*, Rev. Int. Hautes Temper. et Refract. **7**, 335-340 (1970).
12. A. J. Walter, R. M. Dell, K. E. Gilchrist, and R. Taylor, *A comparative study of the thermal diffusivities of stainless steel, hafnium, and Zircaloy*, High Temp.-High Press. **4**, 439-446 (1972).
13. M. Murabayashi, S. Tanaka, and Y. Takahashi, *Thermal Conductivity and Heat Capacity of Zircaloy-2, -4, and Unalloyed Zirconium*, J. Nucl. Sci. And Tech. **12**, 661-662 (1975).
14. R. E. Taylor, private communication to K. D. Maglic, reported in K. D. Maglic, N. Lj. Perovic, and A. M. Stanimirovic, *Calorimetric and Transport Properties of Zircalloy 2, Zircalloy 4, and Inconel 625*, Int. J. of Thermophys. **15**, 741-755 (1994).
15. K. D. Maglic, N. Lj. Perovic, and A. M. Stanimirovic, *Calorimetric and Transport Properties of Zircalloy 2, Zircalloy 4, and Inconel 625*, Int. J. of Thermophys. **15**, 741-755 (1994).
16. K. E. Gilchrist, *Thermal Property Measurements on Zircaloy-2 and Associated Oxide Layers Up to 1200°C*, J. Nucl. Mater. **62**, 257-264 (1976).
17. K. E. Gilchrist, *Thermal Conductivity of Oxide Deposited on Zircaloy Fuel Tube Material - A Continuation of Previous Work*, J. Nucl. Mater. **82**, 193-194 (1979).
18. I. D. Peggs, A. M. Stadnyk, and D. P. Godin, *Thermophysical Properties of Zirconium-Alloy Fuel-Channel Components*, High Temp.-High Pressures **8**, 441-450 (1976).
19. L. R. Bunnell, J. L. Bates, and G. B. Mellinger, *Some High-Temperature Properties of Zircaloy-Oxygen Alloys*, J. Nucl. Mater. **116**, 219-232 (1983);
20. L. R. Bunnell, J. L. Bates, and G. B. Mellinger, *High-Temperature Properties of Zircaloy-Oxygen Alloys*, **EPRI NP-524**, Research Project 251-1 (1977).
21. A. F. Guillermet, *Critical evaluation of the thermodynamic properties of zirconium*, High Temp. - High Press. **19**, 119-160 (1987).
22. J. K. Fink and L. Leibowitz, *Thermal conductivity of zirconium*, J. Nucl. Mater. **226**, 44-50 (1995).

Table 1 Thermal Conductivity of Zircaloy

Temperature K	Thermal Conductivity $\text{W m}^{-1} \text{K}^{-1}$
300	13.41
400	13.99
500	14.74
600	15.67
700	16.79
800	18.08
900	19.55
1000	21.21
1100	23.04
1200	25.05
1300	27.24
1400	29.61
1500	32.16
1600	34.89
1700	37.80
1800	40.89

Table 2 Thermal Conductivity Measurements

Experimenter	Year	Temperature K	No. of Points	Variance		Material, Comments Zr-2 =Zircaloy-2; Zr-4=Zircaloy-4)
				MAT- PRO	Quad- ratic	
C. F. Lucks & H. W. Deem [1]	1958	293-1100	9	0.11	0.32	Zr-2, used in obtaining MATPRO eq.
J. N. Chirigos et al. [2]	1961	373 -1100	9	2.18	2.13	Zr-4, used in obtaining MATPRO eq.
A. E. Powers [3]	1961	293-1100	8	1.83	1.03	Zr-2, used in obtaining MATPRO eq.
			8	0.70	0.54	Zr-4, used in obtaining MATPRO eq.
W. K. Anderson et al. [4]	1962	380-900	6	0.10	0.21	Zr-2, used in obtaining MATPRO eq.
P. B. Scott [5]	1965	350-1100	18	1.46	2.10	Zr-4, used in obtaining MATPRO eq.
A. D. Feith [6]	1966	600 -1800	53	0.96	1.33	Zr-4, used in obtaining MATPRO eq.
E. G. Price, R. W. Mills et al. (AECL data) [7-9]	1980 1997	300-700	5	0.30	0.49	AECL1 Zr-2 cold-worked tube, axial
			5	0.64	1.31	AECL2 Zr-2 annealed strip, rolling
			5	0.13	0.55	AECL3 Zr-2 thin-wall tube, axial
			5	8.95	8.66	AECL4 Zr-2 cold-worked tube
			5	2.03	2.83	AECL5 Zr-2 annealed strip, transverse
			5	2.31	3.15	AECL6 Zr-2 stress-rel.thin-wall tube, circ.
			5	4.26	5.91	AECL7 Zr-2 annealed rod
China: Institute of Atomic Energy [7]	1997	293-1400	23	1.86	0.93	Zr-2 tube 0.65 mm thick, 10 mm d, radial
			23	0.70	0.40	Zr-4 rod, axial

Table 3 Thermal Diffusivity Measurements Included in Analysis

Experimenter	Year	Temperature K	No. of Points	Variance		Material, Comments, Sample thickness (Zr-2 =Zircaloy-2; Zr-4=Zircaloy-4)
				MAT- PRO	Quad- ratic	
A. J. Walter et al. [12]	1972	300-800	6	0.87	0.16	Zr-2, transverse 2.05 mm, Harwell, infrared detector
			6	1.78	0.62	Zr-2, normal, 2.05 mm, Harwell, infrared detector
			6	1.20	0.34	Zr-2, rolling, 2.0 mm, Harwell, infrared detector
			6	1.32	0.27	Zr-2, 2.06 mm, Manchester, infrared dectector
			6	0.81	0.09	Zr-2, 1.04 mm, Manchester, infrared dectector
			6	1.07	0.22	Zr-2, 0.63 mm, Manchester, infrared dectector
M. Murabayashi et al. [13]	1975	300-900	14	0.59	0.04	Zr-2, 2mm
			10	1.99	0.91	Zr-2, 0.6 mm
			19	1.24	0.53	Zr-4, 2 mm
K. E. Gilchrist [16]	1976	298-1500	18	2.47	2.67	Zr-2, 2.5 mm, 1.97 mm
E. G. Price, R. W. Mills et al. (AECL data) [7-9]	1980 1997	290-673	5	0.53	0.02	AECLd1 Zr-2, cold-worked tube, radial
			5	1.20	0.55	AECLd2 Zr-2, annealed strip, through thickness
			5	4.01	5.49	AECLd3 Zr-2, annealed rod, axial,
R. E. Taylor [14]	1991	300-1500	10	1.11	1.32	Zr-4
K. D. Maglic et al. [15]	1994	298-1373	84	0.89	0.65	Zr-2, annealed sheet
			154			Zr-4, 1.7 mm thick, annealed sheet

Table 4 Thermal Conductivity & Diffusivity Data Included in Final Analysis

Experimenter	Year	Temperature K	No. of Points	Variance			Property, Material, Comments (λ =conductivity; D=diffusivity; Zr-2 =Zircaloy-2; Zr-4=Zircaloy-4)
				MATPRO	Quad- ratic	Cubic	
Lucks & Deem [1]	1958	293-1100	9	0.11	0.33	0.29	λ , Zr-2, included in MATPRO analysis
Chirigos et al. [2]	1961	373 -1125	9	2.18	2.32	2.47	λ , Zr-4, included in MATPRO analysis
Powers [3]	1961	293-1100	8	1.83	0.83	0.82	λ Zr-2, included in MATPRO analysis
			8	0.70	0.58	0.61	λ Zr-4, included in MATPRO analysis
Anderson et al. [4]	1962	380-900	6	0.10	0.27	0.22	λ Zr-2, included in MATPRO analysis
Scott [5]	1965	350-1100	18	1.46	2.47	2.31	λ Zr-4, included in MATPRO analysis
Feith [6]	1966	600 -1800	52	0.96	1.21	1.09	λ Zr-4, included in MATPRO analysis, bad datum at 925K not included
Walter et al. [12]	1972	300-800	6	0.87	0.07	0.12	D, Zr-2, transverse 2.05 mm,
			6	1.78	0.40	0.52	D, Zr-2, normal, 2.05 mm,
			6	1.20	0.19	0.26	D, Zr-2, rolling, 2.0 mm,
			6	1.32	0.13	0.19	D, Zr-2, 2.06 mm,
			6	0.81	0.03	0.05	D, Zr-2, 1.04 mm,
			6	1.07	0.10	0.15	D, Zr-2, 0.63 mm,

Table 4 Thermal Conductivity & Diffusivity Data Included in Final Analysis

Experimenter	Year	Temperature K	No. of Points	Variance			Property, Material, Comments (λ =conductivity; D=diffusivity; Zr-2 =Zircaloy-2; Zr-4=Zircaloy-4)
				MATPRO	Quad- ratic	Cubic	
Murabayashi et al. [13]	1975	300-900	14	0.59	0.04	0.08	D, Zr-2, 2 mm
			10	1.99	0.59	0.68	D, Zr-2, 0.6 mm
			19	1.24	0.28	0.31	D, Zr-4, 2 mm
Price [7, 8] Mills et al. [7, 9]; (AECL data)	1980 1997	300-700	5	0.30	0.77	0.71	λ , AECL1, Zr-2 cold-worked tube, axial
			5	0.64	1.68	1.54	λ , AECL2, Zr-2 annealed strip, rolling
			5	0.13	0.75	0.65	λ , AECL3, Zr-2 stress-relieved tube, axial
Price [7, 8] Mills et al. [7, 9]; (AECL data)	1980 1997	290-673	5	0.53	0.06	0.10	D, AECLd1 Zr-2 cold-work tube, radial
			5	1.20	0.29	0.34	D, AECLd2 Zr-2; annealed strip, through thickness
Taylor [14]	1991	300-1500	10	1.11	1.17	1.10	D, Zr-4
Maglic et al. [15]	1994	298-1373	53	0.89	0.37	0.38	D, Zr-2 & Zr-4; reduced to 53 points by averaging data at same temperature
China: Institute of Atomic Energy [7]	1997	293-1400	23	1.86	0.70	0.78	λ , Zr-2 tube, radial
			23	0.70	0.26	0.23	λ , Zr-4 rod, axial

Fig. 1 Recommended Equation for Zircaloy Thermal Conductivity

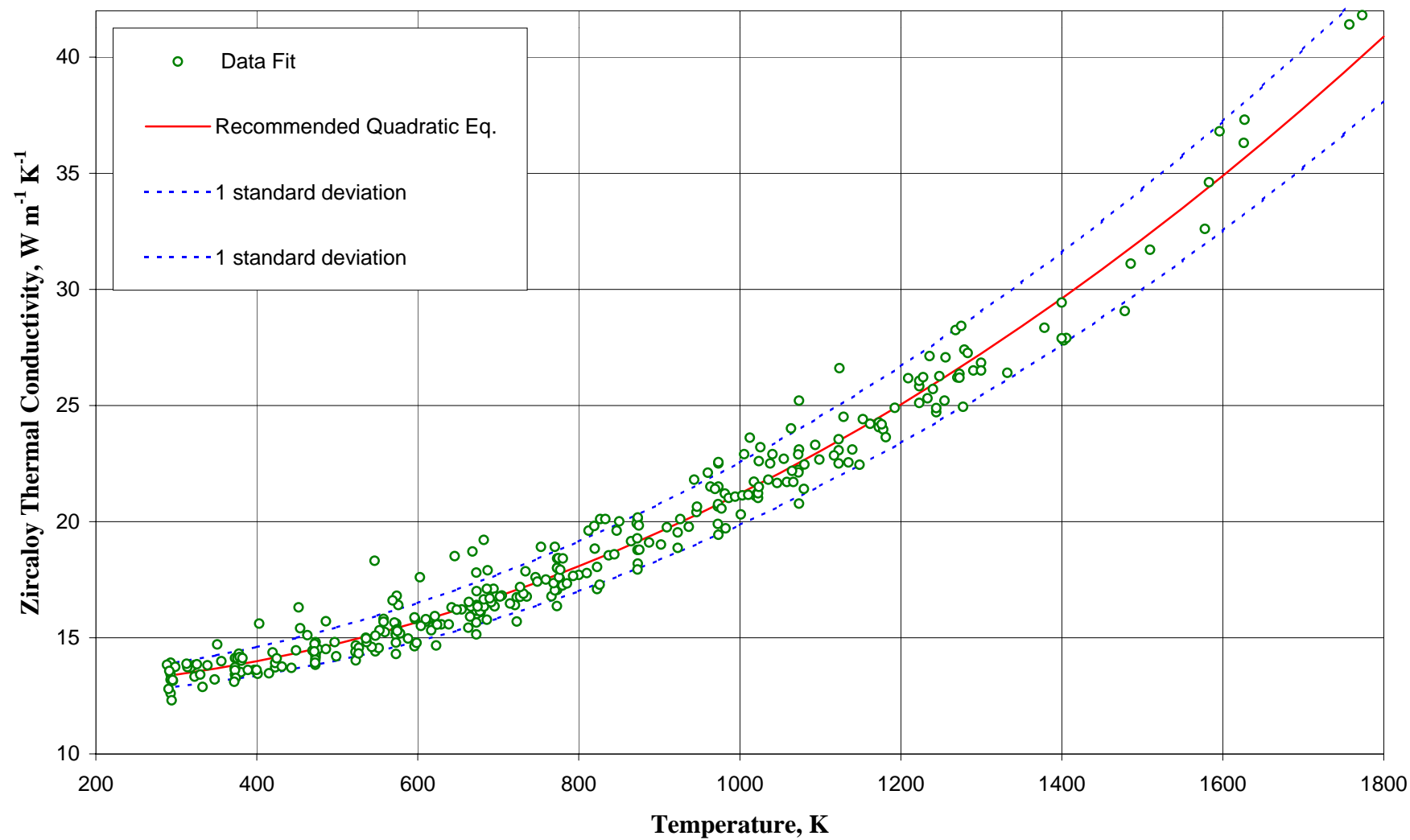


Fig. 2 Comparison of MATPRO Equation with Data Analyzed in MATPRO

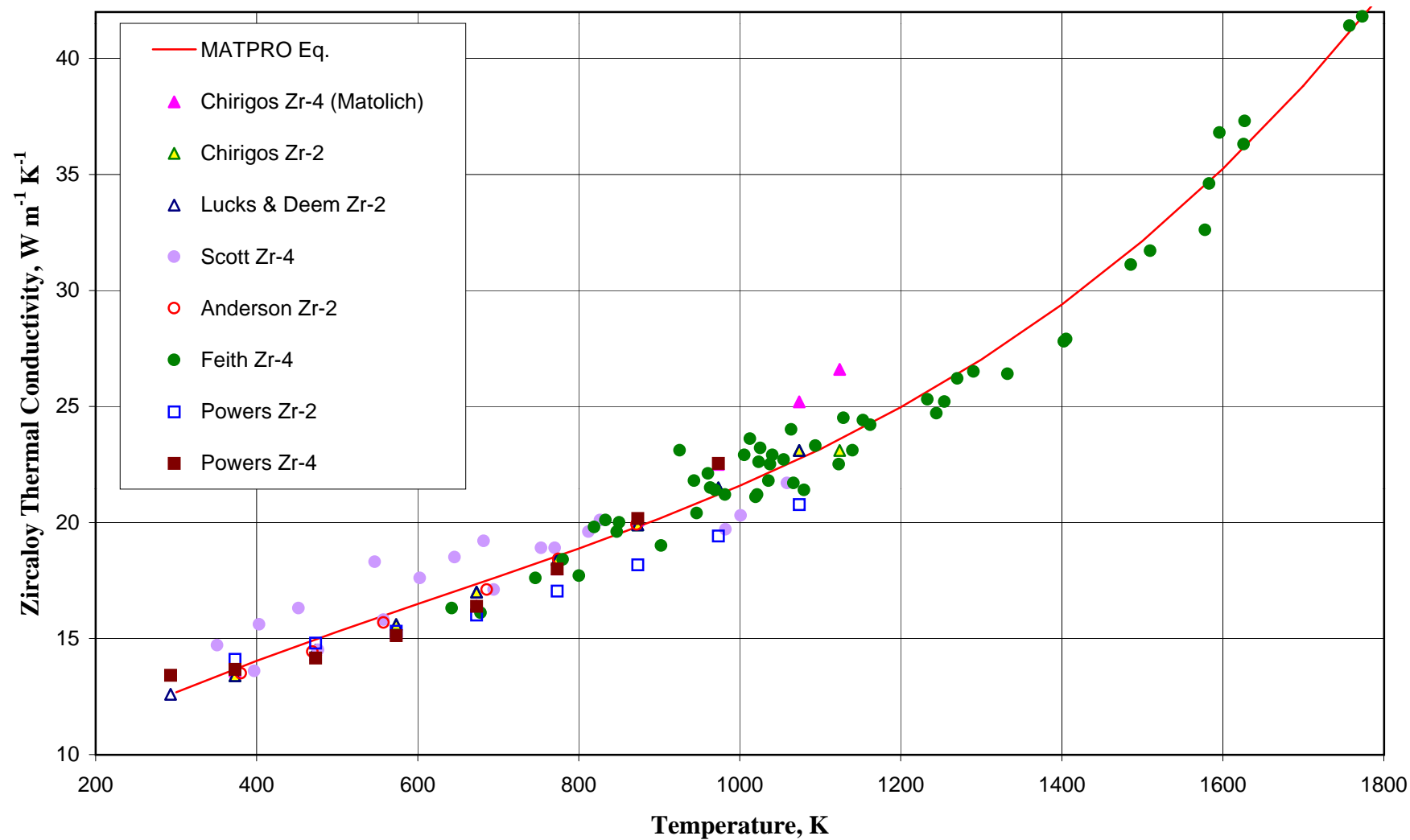


Fig. 3 Comparison of Zircaloy Thermal Conductivity Data with MATPRO Eq.

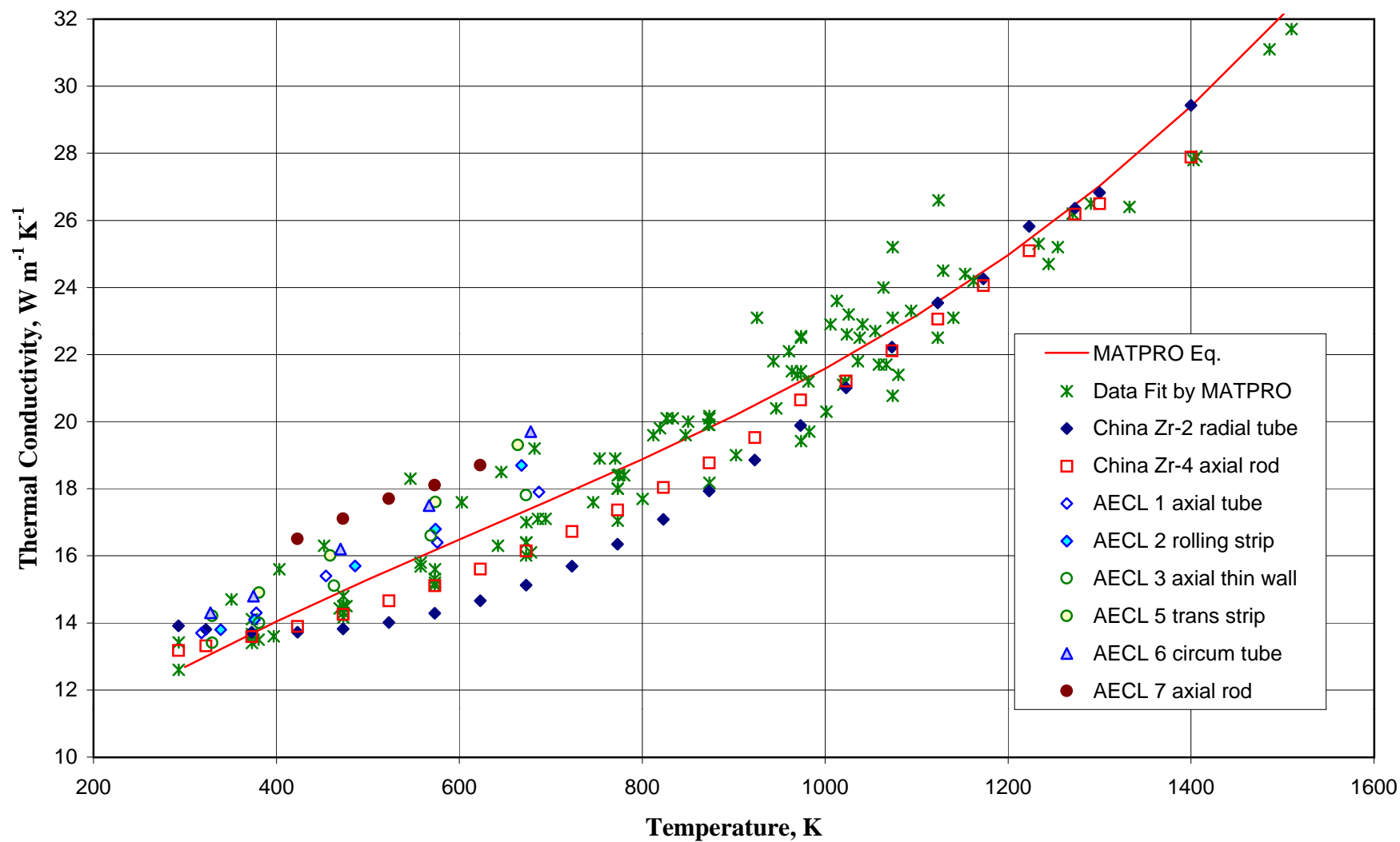


Fig. 4 Study of Effects of Thickness and Direction on Zircaloy Thermal Diffusivity by Walter et al. [12]

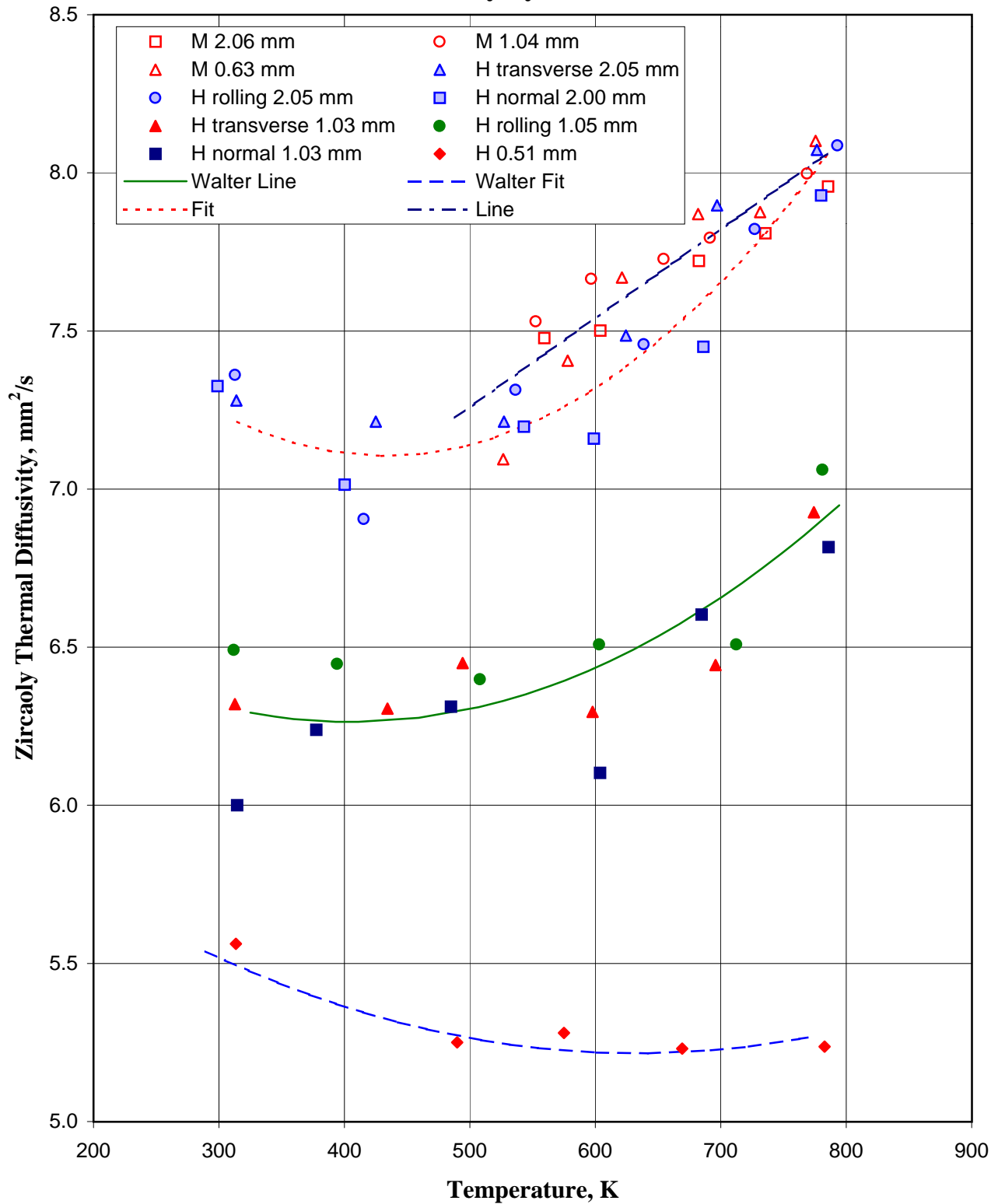


Fig. 5 Zircaloy Thermal Diffusivity Data Considered in this Analysis

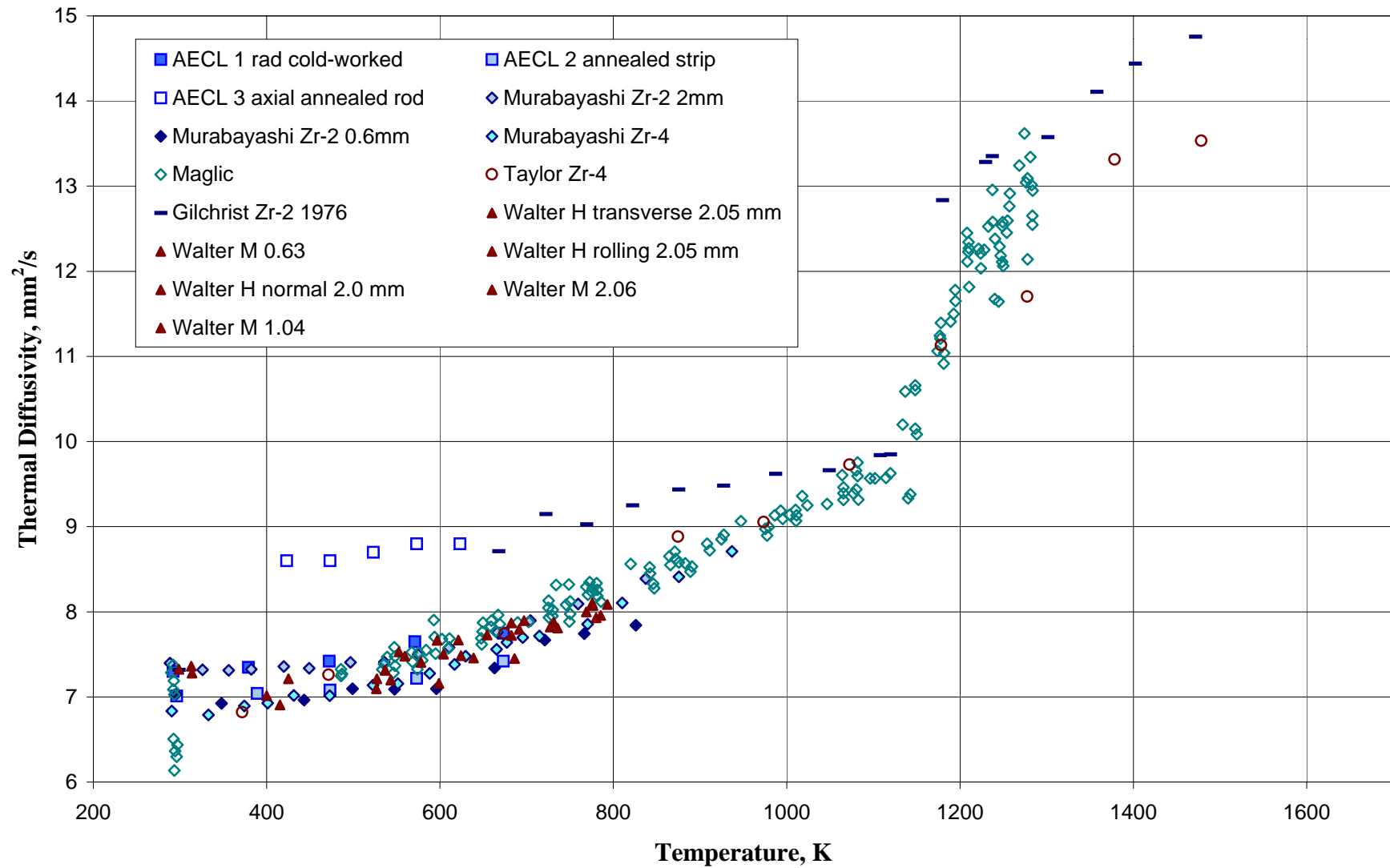


Fig. 6 Comparison of Low-Temperature Zircaloy Thermal Diffusivity Data

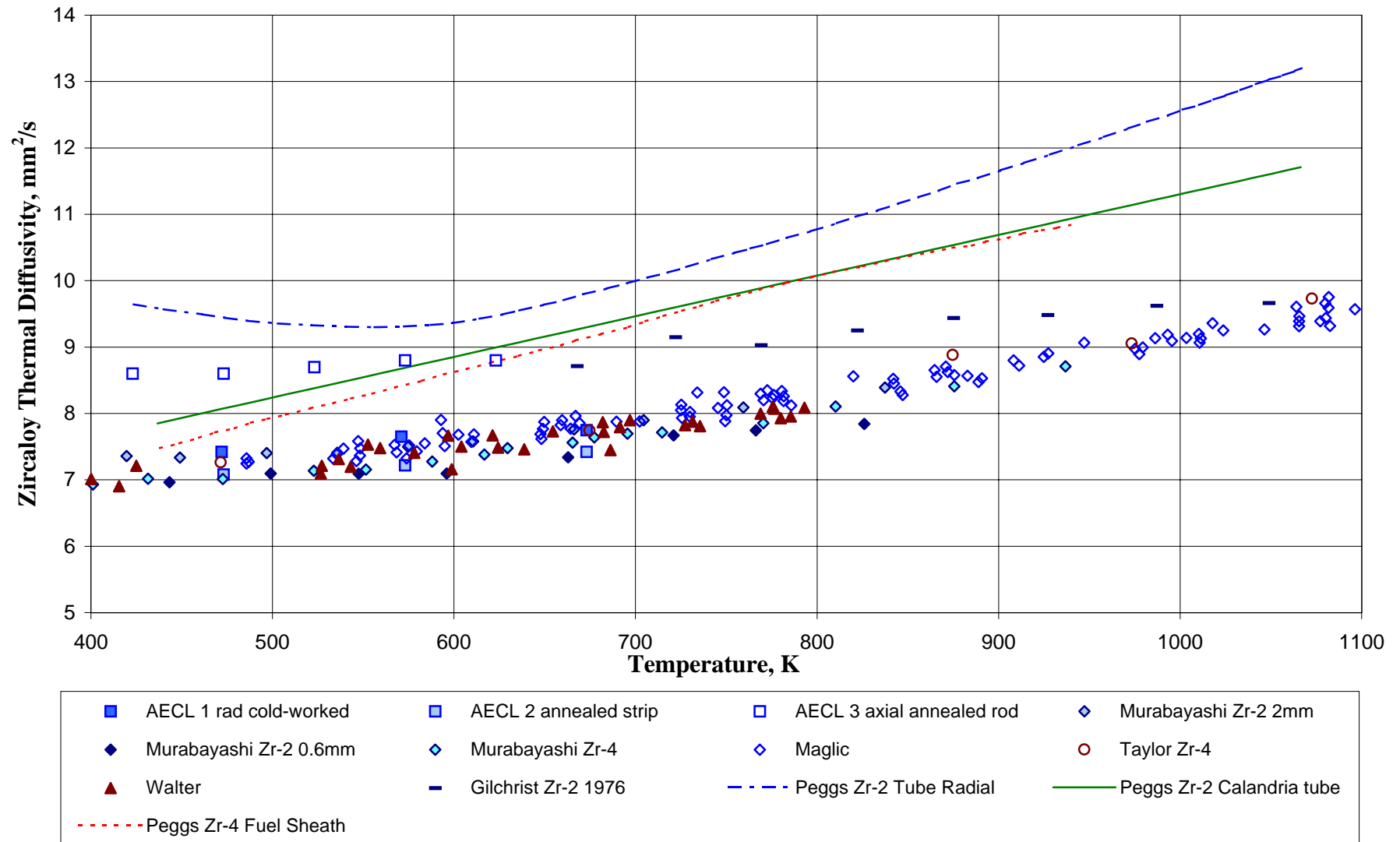


Fig. 7 Comparison of Thermal Diffusivity Results of Bunnell et al. with Other Data

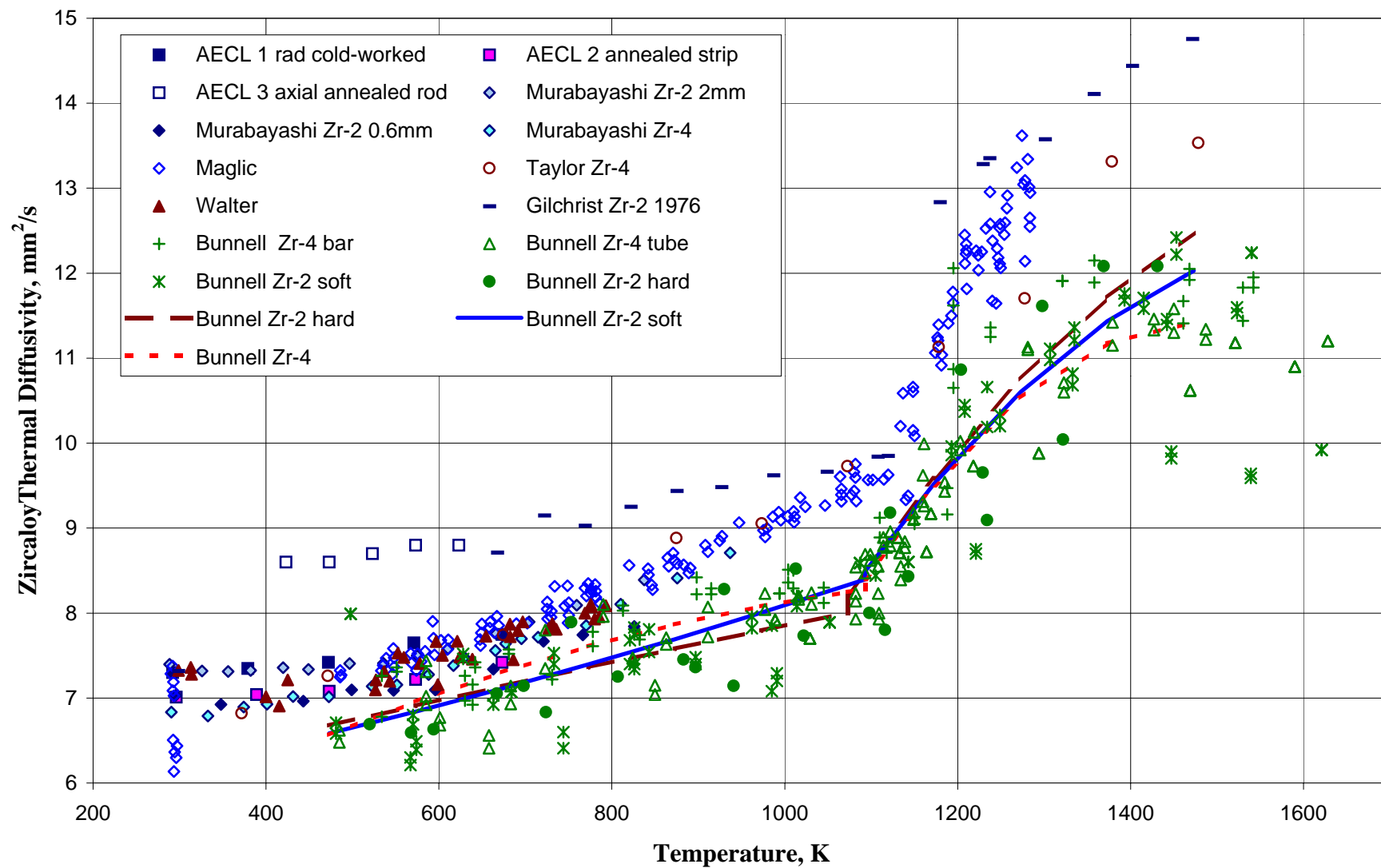


Fig. 8 Zircaloy Thermal Conductivity and Diffusivity Measurements

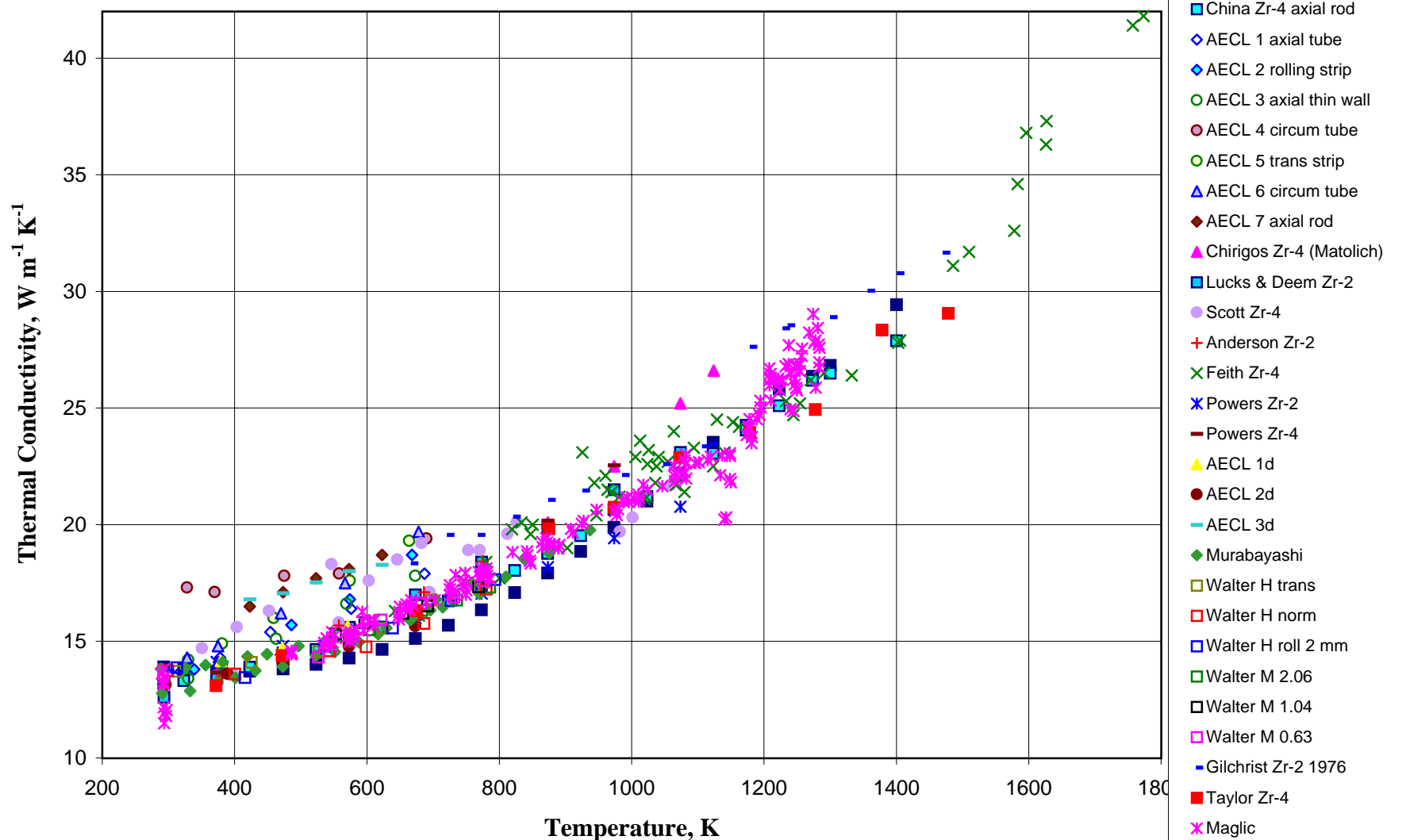


Fig. 9 Comparison of MATPRO Eq. with Thermal Conductivity & Diffusivity Data

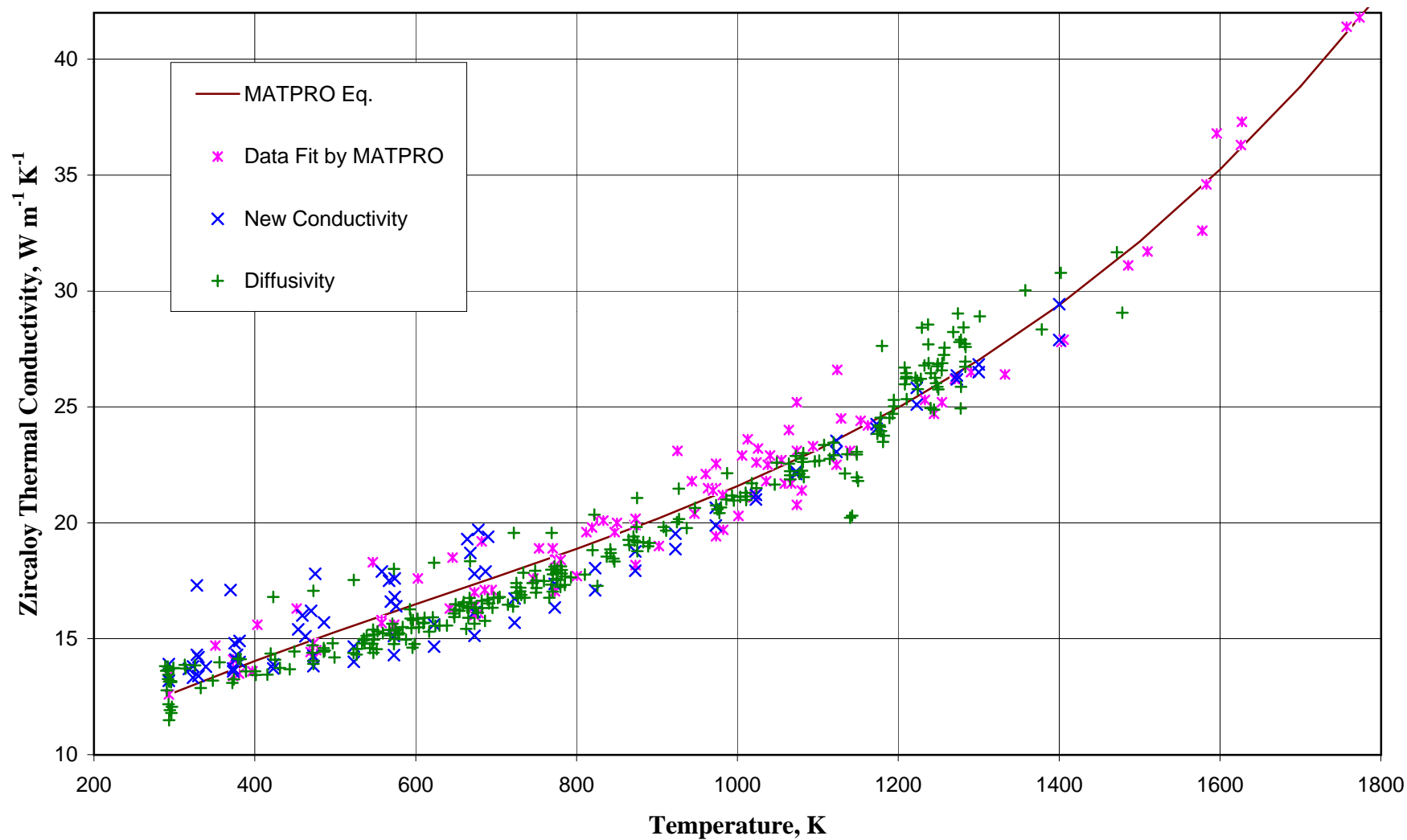


Fig. 10 Comparison of Data with Quadratic Fit and 2 Standard Deviations

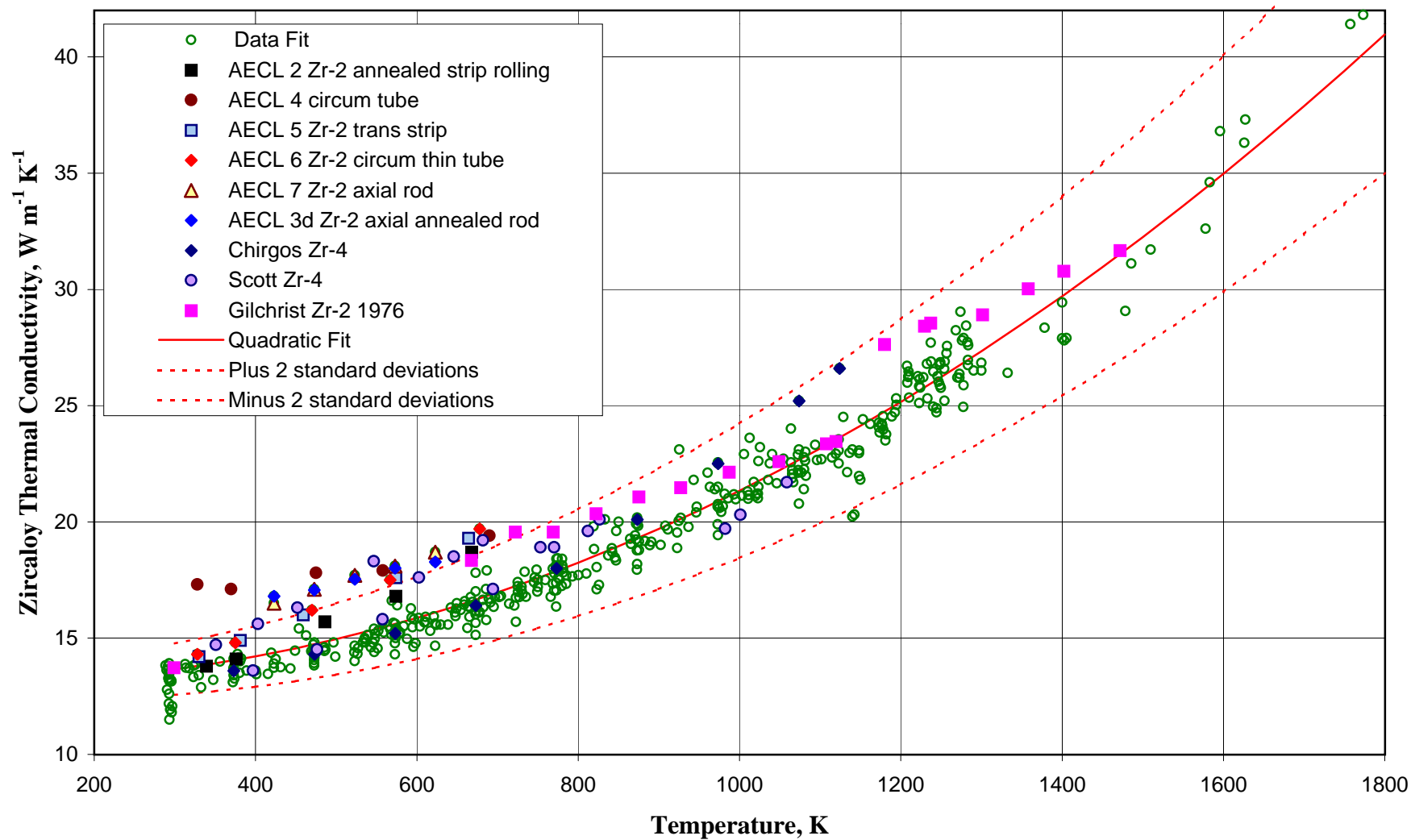


Figure 11 Comparison of Zircaloy Thermal Conductivity Data Not Included in Final Analysis with Quadratic Line Through All the Data

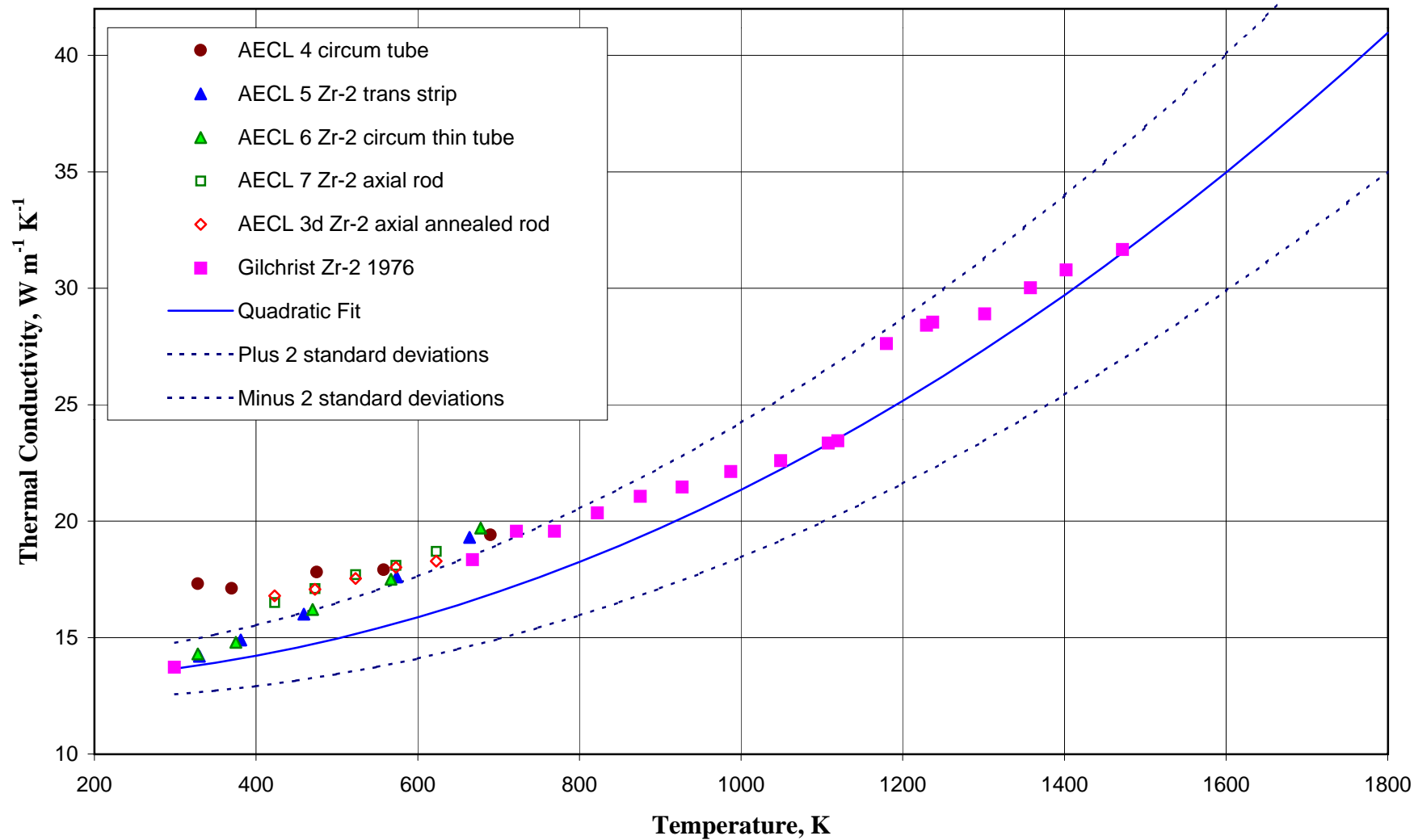


Fig. 12 Comparison of Zircaloy Data with Equations

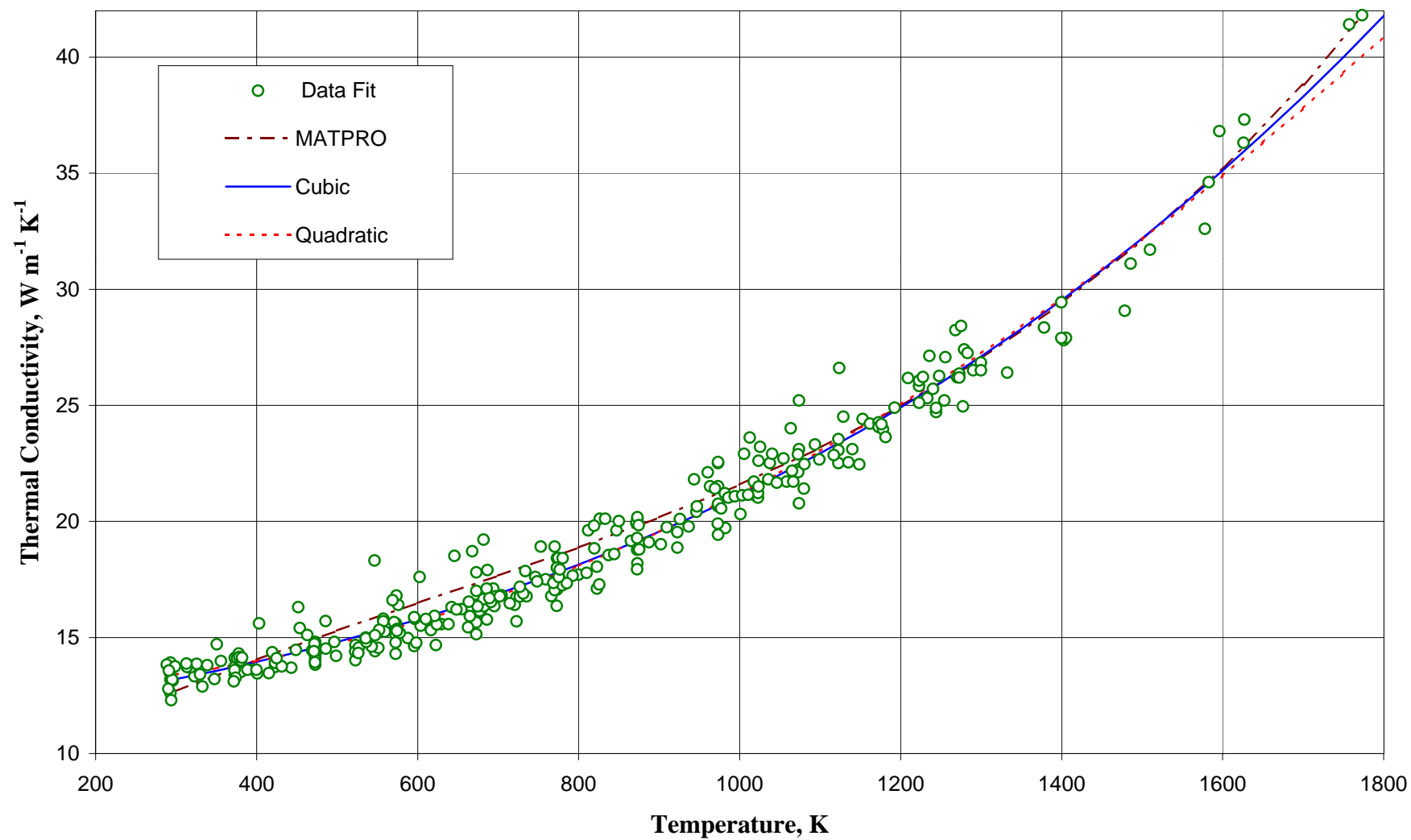


Fig. 13 Deviation of Zircaloy Data from Cubic and Quadratic Equations

